Millimeter Observations of GRB 030329: Continued Evidence for a Two-Component Jet

Kartik Sheth[1,2], Dale A. Frail [3], Stephen White[4], Mousumi Das[4], Frank Bertoldi [5], Fabian Walter[3], Shri R. Kulkarni[1], Edo Berger[1]

ABSTRACT

We present the results of a dedicated campaign on the afterglow of GRB 030329 with the millimeter interferometers of the Owens Valley Radio Observatory (OVRO), the Berkeley-Illinois-Maryland Association (BIMA), and with the MAMBO-2 bolometer array on the IRAM 30-m telescope. These observations allow us to trace the full evolution of the afterglow of GRB 030329 at frequencies of 100 GHz and 250 GHz for the first time. The millimeter light curves exhibit two main features: a bright, constant flux density portion and a steep power-law decline. The absence of bright, short-lived millimeter emission is used to show that the GRB central engine was not actively injecting energy well after the burst. The millimeter data support a model, advocated by Berger et al., of a two-component jet-like outflow in which a narrow angle jet is responsible for the high energy emission and early optical afterglow, and a wide-angle jet carrying most of the energy is powering the radio and late optical afterglow emission.

Subject headings: gamma rays: bursts — radio continuum: general — cosmology: observations

1. Introduction

A link between long-duration gamma-ray bursts (GRBs) and the core collapse of massive stars has long been claimed on observational (e.g. Bloom, Kulkarni & Djorgovski 2002;

[1]Division of Mathematical & Physical Sciences, California Institute of Technology, Pasadena, CA 91125

[2]Email: kartik@astro.caltech.edu

[3]National Radio Astronomy Observatory, P.O. BOX 0, Socorro, NM 87801

[4]Department of Astronomy, University of Maryland

[5]Max-Planck-Institut für Radioastronomie, Auf dem Hügel 69, D–53121 Bonn, Germany

Bloom et al. 2002; Price et al. 2002) and theoretical grounds (Woosley 1993; Paczyński 1998; MacFadyen & Woosley 1999), but the recent GRB 030329 has strengthened this association considerably. Optical spectra taken of this event (Stanek *et al.* 2003; Hjorth *et al.* 2003; Kawabata *et al.* 2003) showed the usual power-law continuum from the afterglow, superimposed upon which were lines characteristic of a Type Ic supernova (SN). Designated SN 2003dh, the brightness of this SNe and its broad line widths are strikingly similar to another peculiar Ic SN 1998bw (Patat *et al.* 2001; Maeda *et al.* 2002), or perhaps SN 1997ef (Iwamoto *et al.* 2000). Depending on the degree of asphericity assumed in modeling the explosion, the derived kinetic energies for SN 1998bw and SN 1997ef are in the range of 5-50 foe (1 foe=10^{51} erg). Such events are labeled "hypernovae", an empirical classification to distinguish them from ordinary core collapse SNe with energies of order 1 foe (Iwamoto *et al.* 1998).

While the non-relativistic component of the explosion (as traced by SN 2003dh) may have been hyper-energetic, the relativistic component (as traced by GRB 030329) seems to be sub-energetic. As noted by Granot, Nakar & Piran (2003) and Berger et al. (2003), if the sharp break in the optical light curves at $t = 0.55$ days (Price *et al.* 2003) is due to a jet-like outflow, then the gamma-ray energy released $E_\gamma \sim 0.05$ foe and the X-ray luminosity (at t=10 hrs) $L_X \sim 3\times10^{43}$ erg s^{-1}. These values of E_γ and L_X lie an order of magnitude or more below which most GRBs are tightly clustered (Bloom, Frail & Kulkarni 2003; Berger, Kulkarni & Frail 2003). Outliers in the energy/luminosity distribution are potentially important for exploring the diversity of the GRB phenomena, and how the central engine partitions the explosion energy.

Millimeter detections of gamma ray bursts (GRBs), while difficult to achieve (e.g., Bremer et al. 1998, Shepherd et al. 1998), are a potentially powerful diagnostic of the explosion energy. Since the peak of the synchrotron spectrum is expected to pass through the millimeter band on a time scale of a day or so after the burst (Sari, Piran & Narayan 1998), such observations are useful for constraining the peak of the spectrum, a quantity that is difficult to obtain by other means. When combined with broadband data these millimeter observations have been especially useful in deriving the kinetic energy of the outflow and the density structure of the circumburst environment (Galama *et al.* 2000; Berger *et al.* 2000; Harrison *et al.* 2001; Yost *et al.* 2002).

In this paper we present measurements of GRB 030329 at 100 GHz made with the millimeter interferometers of the Owens Valley Radio Observatory (OVRO) and the Berkeley-Illinois-Maryland Association (BIMA), and measurements at 250 GHz made with MAMBO-2 bolometer array on the IRAM 30 m telescope. At z=0.1686 (Caldwell *et al.* 2003) this is the closest known GRB and subsequently the flux density at millimeter wavelengths was more

than ten times brighter than any previous event. These observations allow us to trace the full evolution of the afterglow at millimeter wavelengths for the first time. In §2 we discuss the observations and calibration issues, in §3 and §4 we present the results in the form of a light curve and discuss possible interpretations.

2. Observations & Data Reduction

Millimeter Interferometers: We used the Owens Valley Radio Observatory's millimeter array and the Berkeley-Illinois-Maryland Association millimeter array to observe the GRB 030329 in a dedicated campaign beginning 2003 March 30 through 2003 April 17. An additional observation was obtained on 2003 April 30.

For the first three nights, when the redshift of the GRB was unknown, we tuned the local oscillator to the CS(2-1) line at a frequency of 97.98 GHz. After that, we tuned to the CO(J=1-0) line redshifted to z=0.1686.

We imaged the continuum flux using the analog correlator at OVRO which consists of four 1 GHz bands around the LO frequency from ±0.5-1.5 GHz and ±2.5-3.5 GHz. The array was in the H configuration and the projected baselines ranged from 5.5 to 84.0 kλ and the single-sideband system temperatures ranged from 150 to 400 K. The complex instrumental gain was calibrated using the quasar 1159+292 every 15 minutes. The flux of 1159+292 was determined using 3C 273 since no planets were available for an absolute calibration; hence, the resulting uncertainty in the overall flux scale is ∼15%. We use a flux of 1.95 Jy for 1195+292 to calibrate all the data. The calibrations were done with the MMA software package (Scoville *et al.* 1993) imaged using standard routines in MIRIAD (Sault, Teuben, & Wright 1995).

At BIMA we used the 800 MHz digital correlator to map the GRB. BIMA was in the compact (C) configuration and projected baselines ranged from 2.2–29.3 kλ. The single-sideband temperatures ranged from 200 to 400 K. The same phase calibrator, 1159+292 was used to calibrate the BIMA data. The results for the continuum flux measurements are summarized in Table 1. At OVRO we used the 1 GHz digital spectrometer, and the new 8 GHz COBRA spectrometer, and at BIMA we used the 800 MHz spectrometer both to search for a redshifted CO spectral line in absorption; we did not detect it.

Millimeter continuum flux from the GRB was detected at α(J2000)=$10^h44^m49^s.95$, δ(J2000) = $21^o31'\ 17''.30$. This position is coincident with the radio and optical afterglows. The observing campaign is summarized in Table 1. On the first three days, we were also able to track the evolution of the GRB flux within a scan because it was bright. These data

are listed in Table 2. The light curve is plotted in Figure 1.

MAMBO 250 GHz observations: The millimeter continuum measurements were made using the 117-channel MAMBO-2 array (Kreysa et al. 1999) at the IRAM 30 m telescope on Pico Veleta (Spain). MAMBO-2 has a half-power spectral bandwidth of 210 and 290 GHz with an effective frequency of 250 GHz. The beam size on the sky is 10.7 arcsec. The sources were observed with a single channel using the standard on-off mode with the telescope secondary chopping in azimuth by 32″ at a rate of 2 Hz.

Observations of GRB 030329 were done on eight different epochs between March 30 and April 20, with integration times on sky ranging between 5 and 17 minutes. The observing conditions were good, with the exception of April 2, when the sky noise was unusually strong. The source was observed at elevations between 56 and 74 degrees, with line of sight opacities at 250 GHz in the range 0.1 to 0.3.

The pointing and focus were checked frequently on the quasar 1043+241, which is only 3 degrees away from the GRB. Usually the pointing was found to be stable within $\sim 3''$. For the absolute flux calibration a number of calibration sources were observed, mostly CW-Leo, which is near the target. We used a flux calibration factor of 35,000 counts per Jansky, the one sigma uncertainty of which we estimated to be 10%.

The data were analyzed using the MOPSI software package. Correlated noise was subtracted from each channel using the weighted average signals from the surrounding channels. These data are listed in Table 3 and the light curve is plotted in Figure 1.

3. Results

The 100 GHz and 250 GHz millimeter light curves in Figure 1 exhibit two main features: a bright, constant flux density portion and a steep decline. A power-law fit to the decay gives $\alpha_R = -1.98$ (where $F_\nu \propto t^\alpha$) at 100 GHz and $\alpha_R = -1.68$ at 250 GHz. These values are in excellent agreement with that derived by Price et al. (2003) for the optical decay beyond $\sim$0.5 days ($\alpha_\circ = -1.97 \pm 0.12$) and suggests a common physical effect.

The second feature of the light curves in Figure 1 is the bright flux density plateau. In the first week after the burst we derive a mean flux density at 100 GHz of 58 mJy. The emission is constant during this time expect for a two day period starting April 2 where there is a small ($< 20\%$) but significant drop in the flux density followed by a rise to its mean level on April 5. Likewise, the mean flux density at 250 GHz for the first 4 epochs prior to the decay is 44 mJy. Small variations at 250 GHz during this time are likely due to

uncertainties in the calibration.

During the time that these millimeter measurements were made the the optical light curve had a prominent bump at Δt=1.5 days with the flux increasing by a factor of two. There may be a second bump at 3.5 days, but this interpretation depends on whether we compare to a power law with $\alpha = -2$ or -1. In order to search for similar variations at 100 GHz we subdivided each of our observing sessions into 2-hour intervals. The results of this analysis are summarized in Table 2. With the exception of a possible increase by about 10 mJy ($15 - 20\%$) at $t \approx 0.7$ d and $t \approx 2.8$ d, neither of which corresponds to a change in the optical brightness, we find no significant variations.

4. Discussion

Two explanations have been offered as to why GRB 030329 appears to be under-energetic compared to other GRBs. Granot et al. (2003) have explained the observed steep decay in the optical light curves of GRB 030329 at $t = 0.55$ days (Price *et al.* 2003) in terms of a standard model of a jet expanding into a constant density medium (Sari, Piran & Halpern 1999). Note that such steep temporal breaks $\Delta\alpha > 1$ are not expected in spherical outflows in general, nor are they expected in collimated outflows expanding into a wind-blown medium (Sari et al. 1998; Kumar & Panaitescu 2000). In their model the fluctuations in the optical light curve (§3) originate from "refreshed shocks", in which slower moving ejecta catch up with the main shock and re-energize it. In this picture energy injection from the central engine is not instantaneous (as commonly assumed) but episodic, with most of the energy being carried by ejecta with the lower Lorentz factors.

An unavoidable consequence of having the GRB central engine inject a range of Lorentz factors Γ over time, instead of a single high Lorentz factor shell, is that each newly arrived shell at the shock front modifies the afterglow spectrum, producing a short-lived reverse shock, and shifts the combined spectrum to lower frequencies (Rees & Mészáros 1998; Kumar & Piran 2000). According to the more detailed calculations of Sari & Mészáros (2000), which take into account synchrotron self-absorption, there should be a significant enhancement of the flux density at millimeter and submillimeter wavelengths. Short-lived reverse shocks increase the peak flux density by Γ and shift the peak to lower frequencies by a factor Γ^{-2}. For the Lorentz factors given by Granot et al. (2003) we would have expected to see order of magnitude variations in the millimeter flux decaying on timescales of a day or less. This key prediction is contrary to what was seen (§3) in our millimeter data and thus our observations rule out the refreshed shock model.

Berger et al. (2003) proposed a two component jet model based on the existence of two different jets breaks, one in the optical light curves at 0.55 days and another best seen in the radio light curves at 9.8 days. Single-jet fits to the radio data could not explain the evolution of the optical emission before 1.5 days, especially the sharp break at 0.55 days (Price et al. 2003). The millimeter observations presented here are crucial in this respect since they define the peak of the synchrotron spectrum and hence the overall normalization. Lacking such data, earlier claims of a two component outflow for GRB 991216 (Frail *et al.* 2000) are less secure. In this case Berger et al. (2003) define a narrow angle jet with $t_{NAJ} = 0.55$ days and $\theta_{NAJ} = 0.09$ rad which is responsible for the early afterglow, and a wide angle jet $t_{WAJ} = 9.8$ days and $\theta_{WAJ} = 0.3$ rad which carries the bulk of the energy in the outflow and dominates the optical and radio emission after ~ 1.5 days. It is likely that the plateau, seen in the millimeter light curves (§3) during the first week, is a combination of the falling flux density (as $t^{-1/3}$) from the NAJ, and a rising flux density (as $t^{1/2}$) from the WAJ (Sari et al. 1999).

Since in the two-component model the flux increase at 1.5 d is due to the rise of the wide-jet component, which then evolves in the usual fashion as $F_\nu \propto t^{-1}$, the subsequent possible fluctuations discussed by Granot et al. (2003) and in §3 are modest and no longer require refreshed shocks but instead could be explained by variations in the circumburst density.

In summary, the millimeter observations presented here have been used to distinguish between two equally compelling models for GRB 030329 and its afterglow. The absence of bright, short-lived millimeter emission, coincident with "bumps" in the optical light curve between 1 and 7 days after the burst, was used to show that the GRB central engine was not actively injecting energy on this timescale. Instead, the millimeter data support the proposed two-component jet. It is possible that the true structure of GRB outflows are considerably more complicated than the simple picture presented here (Zhang & Mészáros 2002; Rossi, Lazzati & Rees 2002; Perna, Sari & Frail 2003). Models of relativistic jets propagating out through the stellar progenitor show that there may exist a large range in Lorentz factors in the outflow (MacFadyen, Woosley & Heger 2001; Zhang, Woosley & MacFadyen 2003), which decrease away from the rotation axis as the degree of baryon entrainment increases. Nonetheless, within the limits of the current data for GRB 030329, there is evidence for jet structure with at least two distinct components, with the wider of the two carrying the bulk of the energy. This last point is worth emphasizing since events like GRB 030329/SN 2003dh and GRB 980425/SN 1998bw (Kulkarni *et al.* 1998) have shown that the group of sub-energetic bursts may simply be an artifact of limited observations. True calorimetry of GRBs must account for material at low Lorentz factors (Berger *et al.* 2003), which typically are brightest at radio and optical wavelengths.

GRB research at Caltech is supported by grants from NASA and the National Science Foundation. The National Radio Astronomy Observatory is a facility of the National Science Foundation operated under cooperative agreement by Associated Universities, Inc. DAF thanks the Astronomical Institute at the University of Amsterdam for their hospitality during the time when this paper was written. Research at the OVRO is partially funded by NSF grant AST-9981546, and at BIMA by NSF grant AST-9981289.

REFERENCES

Berger, E., Kulkarni, S. R., and Frail, D. A. 2003, ApJ, 590, 379.

Berger, E. *et al.* 2000, ApJ, 545, 56.

Berger, E. *et al.* 2003, Nature, submitted.

Bloom, J. S., Frail, D. A., and Kulkarni, S. R. 2003, ApJ submitted, astro-ph/0302210.

Bloom, J. S., Kulkarni, S. R., and Djorgovski, S. G. 2002, AJ, 123, 1111.

Bloom, J. S. *et al.* 2002, ApJ, 572, L45.

Bremer, M., Krichbaum, T. P., Galama, T. J., Castro-Tirado, A. J., Frontera, F., Van Paradijs, J., Mirabel, I. F., and Costa, E. 1998, A&A, 332, L13.

Caldwell, N., Garnavich, P., Holland, S., Matheson, T., and Stanek, K. Z. 2003, GRB Circular Network, 2053, 1.

Frail, D. A. *et al.* 2000, ApJ, 538, L129.

Galama, T. J. *et al.* 2000, ApJ, 541, L45.

Granot, J., Nakar, E., and Piran, T. 2003, ApJ, submitted; astro-ph/0304563.

Harrison, F. A. *et al.* 2001, ApJ, 559, 123.

Hjorth, J. *et al.* 2003, Nature, in press.

Iwamoto, K. *et al.* 1998, Nature, 395, 672.

Iwamoto, K. *et al.* 2000, ApJ, 534, 660.

Kawabata *et al.* 2003, ApJ, submitted; astro-ph/0306155.

Kreysa, E. *et al.* 1999, Infrared Physics and Technology, 40, 191.

Kulkarni, S. R. *et al.* 1998, Nature, 395, 663.

Kumar, P. and Panaitescu, A. 2000, ApJ, 541, L9.

Kumar, P. and Piran, T. 2000, ApJ, 532, 286.

MacFadyen, A. I. and Woosley, S. E. 1999, ApJ, 524, 262.

MacFadyen, A. I., Woosley, S. E., and Heger, A. 2001, ApJ, 550, 410.

Maeda, K., Nakamura, T., Nomoto, K., Mazzali, P. A., Patat, F., and Hachisu, I. 2002, ApJ, 565, 405.

Paczyński, B. 1998, ApJ, 494, L45.

Patat, F. *et al.* 2001, ApJ, 555, 900.

Perna, R., Sari, R., and Frail, D. A. 2003, ApJ, in press; astro-ph/0305145.

Price, P. A. *et al.* 2002, ApJ, 572, L51.

Price, P. A. *et al.* 2003, Nature in press.

Rees, M. J. and Mészáros, P. 1998, ApJ, 496, L1.

Rossi, E., Lazzati, D., and Rees, M. J. 2002, MNRAS, 332, 945.

Sari, R. and Mészáros, P. 2000, ApJ, 535, L33.

Sari, R., Piran, T., and Halpern, J. P. 1999, ApJ, 519, L17.

Sari, R., Piran, T., and Narayan, R. 1998, ApJ, 497, L17.

Sault, R. J., Teuben, P. J., and Wright, M. C. H. 1995, in ASP Conf. Ser. 77: Astronomical Data Analysis Software and Systems IV, 433.

Scoville, N. Z., Carlstrom, J. E., Chandler, C. J., Phillips, J. A., Scott, S. L., Tilanus, R. P. J., and Wang, Z. 1993, PASP, 105, 1482.

Shepherd, D. S., Frail, D. A., Kulkarni, S. R., and Metzger, M. R. 1998, ApJ, 497, 859.

Stanek, K. Z. *et al.* 2003, ApJ, 591, L17.

Woosley, S. E. 1993, ApJ, 405, 273.

Yost, S. A. *et al.* 2002, ApJ, 577, 155.

Zhang, B. and Mészáros, P. 2002, ApJ, 571, 876.

Zhang, W., Woosley, S. E., and MacFadyen, A. I. 2003, ApJ, 586, 356.

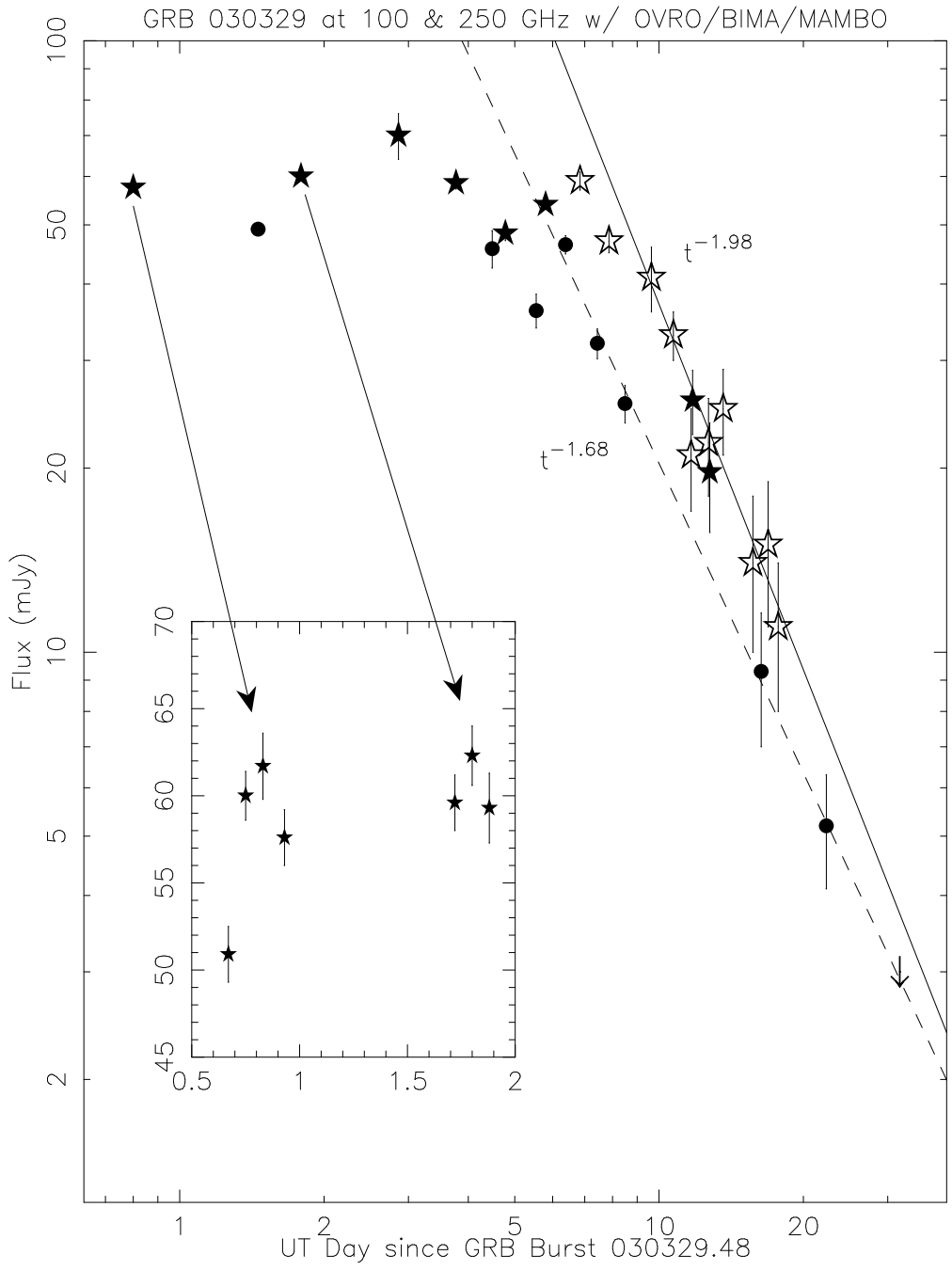

Fig. 1.— Millimeter flux as a function of time on a logarithmic scale. The stars indicate 100 GHz (3mm) data. Filled stars represent OVRO observations, and the open stars represent BIMA observations. Filled circles represent the 250 GHz, IRAM 30-m MAMBO observations. On two days (2003 April 10 and April 11), both the BIMA and OVRO observatories observed the GRB. The measurements are consistent with each other. The inset shows the measurements from the first two OVRO epochs which have been subdivided into 2-hr intervals to look for flux density variations.

Table 1. Observations

UTDay	Beginning UT	End UT	Flux	1σ Rms	Observatory	Comments
03Mar30	02:32	11:10	57.5	0.8	OVRO	
03Mar31	03:48	09:16	60.0	0.9	OVRO	
03Apr01	05:49	10:47	70	6	OVRO	(uv-avg, terrible weather)
03Apr02	01:22	10:39	58.5	1.3	OVRO	
03Apr03	01:59	10:38	48.4	1.3	OVRO	
03Apr04	04:38	09:01	53.9	0.9	OVRO	
03Apr05	04:43	10:30	59	2	BIMA	
03Apr06	04:49	11:33	47	2	BIMA	
03Apr07	...	...	...	...	OVRO	No data, Bad weather
03Apr08	02:56	03:17	41	5	BIMA	
03Apr09	04:27	04:49	33	3	BIMA	
03Apr10	03:02	03:29	21	4	BIMA	
	04:55	06:10	25.8	3.1	OVRO	
03Apr11	03:44	04:08	22	4	BIMA	
	05:02	06:17	19.7	4.0	OVRO	
03Apr12	01:56	02:25	25	4	BIMA	
03Apr13	...	...	...	...	BIMA	No data, Bad weather
03Apr14	04:07	04:30	14	4	BIMA	
03Apr15	08:30	09:18	15	4	BIMA	
03Apr16	04:40	05:28	11	3	BIMA	
03Apr17	03:48	04:28	...	...	BIMA	No data, Bad weather
...	...	...	...	...	...	Apr 18-30, no obs
03Apr30	04:06	08:15	ND	3	BIMA	Upper limit 3 mJy/bm

Table 2. Early Time Evolution

Day	Beginning UT	End UT	Flux	1σ Rms	Observatory	Comments
03Mar30	02:32	04:32	50.9	1.6	OVRO	
03Mar30	04:32	06:32	60.0	1.4	OVRO	
03Mar30	06:32	08:32	61.7	1.9	OVRO	
03Mar30	08:32	11:10	57.6	1.6	OVRO	
03Mar31	03:48	05:48	59.6	1.6	OVRO	
03Mar31	05:48	07:48	62.3	1.7	OVRO	
03Mar31	07:48	09:16	59.3	2.0	OVRO	
03Apr02	01:22	04:22	55.4	1.8	OVRO	
03Apr02	04:22	07:22	66.5	2.1	OVRO	
03Apr02	07:22	10:39	54.6	2.4	OVRO	

Table 3. 250 GHz MAMBO Observations

Day	Beginning UT	Int (sec)	Flux	1σ Rms	Comments
03Mar30	22:21	1031	49.2	1.1	elev.=74°, τ=0.21
03Apr02	06:55	156	45.7	3.2	elev.=62°, τ=0.36
03Apr02	23:07	308	36.2	2.3	elev.=71°, τ=0.29
03Apr04	00:29	310	41.6	1.6	elev.=56°, τ=0.13
03Apr04	20:39	312	46.4	1.6	elev.=65°, τ=0.13
03Apr05	21:54	306	32.0	1.8	elev.=74°, τ=0.10
03Apr06	23:17	310	25.5	1.8	elev.=67°, τ=0.10
03Apr14	19:30	468	9.3	2.3	elev.=60°, τ=0.26
03Apr20	19:15	970	5.2	1.1	elev.=62°, τ=0.24